

PREPARED FOR SUBMISSION TO JINST

15TH TOPICAL SEMINAR ON INNOVATIVE PARTICLE AND RADIATION DETECTORS (IPRD19)

14-17 OCTOBER 2019

SIENA, ITALY

Search for light dark matter with NEWS-G

Konstantinos Nikolopoulos on behalf of NEWS-G collaboration

*School of Physics and Astronomy, University of Birmingham,
Birmingham, B15 2TT, United Kingdom*

E-mail: k.nikolopoulos@bham.ac.uk

ABSTRACT: The NEWS-G collaboration is searching for light dark matter candidates using a spherical proportional counter. Light gases, such as hydrogen, helium, and neon, are used as targets, providing access in the 0.1–10 GeV mass range. First results obtained with SEDINE, a 60 cm in diameter detector, in the Underground Laboratory of Modane yielded a 90% confidence level upper limit of $4.4 \cdot 10^{37} \text{ cm}^2$ on the nucleon-dark matter interaction cross-section for a candidate with 0.5 GeV mass. Recent developments in several aspects of the detector instrumentation are presented, along with the construction of a new, 140 cm in diameter, detector with new compact shielding.

KEYWORDS: Dark Matter detectors (WIMPs, axions, etc.); Gaseous detectors; Materials for gaseous detectors; Gas systems and purification

Contents

1	Introduction	1
2	The spherical proportional counter	2
3	First NEWS-G results on the search for light DM	2
4	Developments in sensor design	3
4.1	Single-anode sensors	3
4.2	Multi-anode sensors	5
5	A large size spherical proportional counter with compact shielding	5
6	Electroplating for NEWS-G	5
7	Gas purification	7
8	Detector calibration and monitoring	7
9	Summary	8

1 Introduction

It is established from a variety of astrophysical observations [1, 2] and precise measurements of the Cosmological Microwave Background [3] that approximately 84.5% of the matter content of our Universe consists of non-baryonic cold Dark Matter (DM). Although the nature of DM is currently unknown, many theories beyond the Standard Model (SM) predict massive neutral particles, thermally produced in the early Universe, that could account for the observed DM relic density. A generic class of well motivated DM candidates is known as Weakly Interacting Massive Particles (WIMPs) [4]. The WIMP hypothesis favours DM masses in the 10–1000 GeV range [5]. However, the lack of evidence for supersymmetry at the LHC [6] and of convincing evidence from direct and indirect detection experiments motivates the investigation of models with lighter DM candidates and, potentially, more complex couplings — e.g. hidden sectors [7, 8], asymmetric dark matter [9, 10], and more generic descriptions through effective theory [11].

Direct detection experiments aim to detect incoming DM particles from the Milky Way halo via their coherent elastic scattering off a target nuclei. A key element towards improved sensitivity to low mass candidates is the possibility to operate with low energy threshold, dictated by the expected nuclear recoil energy spectrum, which is concentrated to ever lower energies as the DM candidate mass decreases. A further experimental challenge arises from the fact that recoil ions only partially dissipate their kinetic energy as ionisation. The fraction of ion kinetic energy released in

the detector medium through ionisation, the ionisation quenching factor, depends on the ion atomic number and kinetic energy. Sensitivity to low mass DM candidates is further hindered by the rapid decrease of this factor with decreasing kinetic energy, for energies below a few keV [12].

2 The spherical proportional counter

The spherical proportional counter, presented in figure 1, is a novel gaseous detector [13–15]. It consists of a grounded spherical shell which acts as the cathode and a small spherical anode, the sensor, supported at the centre by a grounded metallic rod, to which the high voltage is applied and from which the signal is read-out. In the ideal case the electric field has an $1/r^2$ dependence on the radial distance from the detector centre. This dependence naturally divides the detector into the drift region, where under the influence of the electric field the electrons drift towards the anode, and the amplification region, where charge multiplication occurs.

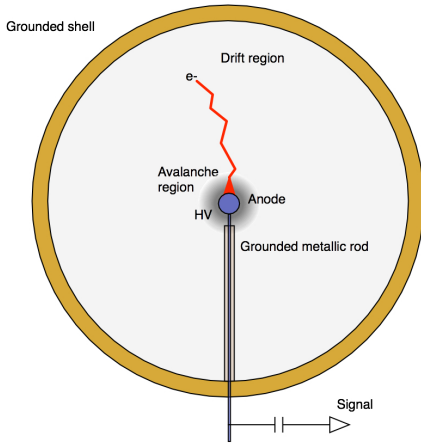


Figure 1. Spherical proportional counter design and principle of operation [15].

The spherical geometry provides several advantages for building large volume detectors. The sphere has the lowest surface-to-volume ratio and is well suited for high pressure operation. Furthermore, light elements exhibit favourable ionisation quenching factor. Overall, the spherical proportional counter exhibits the following key features: a) very low energy thresholds, down to single ionisation electron detection, thanks to small sensor capacitance and high gain operation; b) small number of read-out channels; c) background rejection and fiducialisation through pulse shape analysis; d) simple and robust construction with radiopure materials; e) variety of light target gases, allowing optimisation of momentum transfer for light particles; and f) possibility to vary the operational pressure and high voltage, providing additional handles to disentangle potential signals from unknown backgrounds.

3 First NEWS-G results on the search for light DM

The $\varnothing 60$ cm spherical proportional counter SEDINE, shown in figure 2(a), is installed at the Laboratoire Souterrain de Modane (LSM), which has an overburden of 4800 m water equivalent. The detector is constructed using pure (NOSV) copper, chemically cleaned to remove radon deposits, and a $\varnothing 6.3$ mm spherical anode made of silicon, shown in figure 2(b). In figure 2(c), the shielding of SEDINE is shown, which — moving outwards — comprises 8 cm of copper, 15 cm of lead, and 30 cm of polyethylene. First results were obtained using a Ne/CH₄ (99.3%/0.7%) gas mixture at 3.1 bar pressure, with a total target mass exposure of 9.6 kg · days.

The 90% confidence level (CL) upper limit on the spin-independent DM-nucleon scattering cross section, derived considering all observed events as candidates, is presented in figure 3 as a

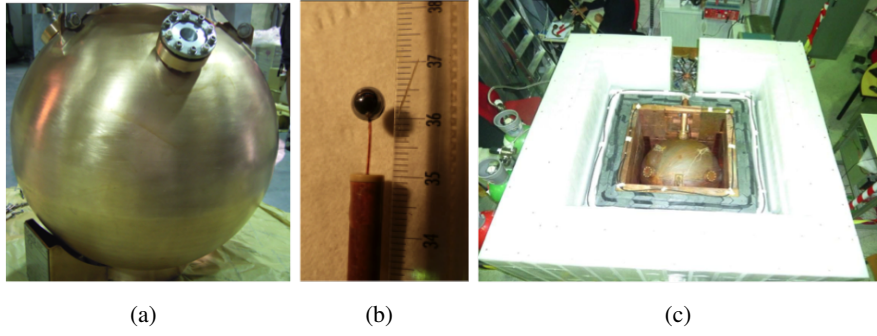


Figure 2. (a) SEDINE, the $\varnothing 60$ cm spherical proportional counter operating at LSM; (b) the $\varnothing 6.3$ mm silicon sensor installed in SEDINE, with a $\varnothing 380$ μm diameter insulated HV wire routed through a grounded copper rod; and (c) the cubic shielding of SEDINE.

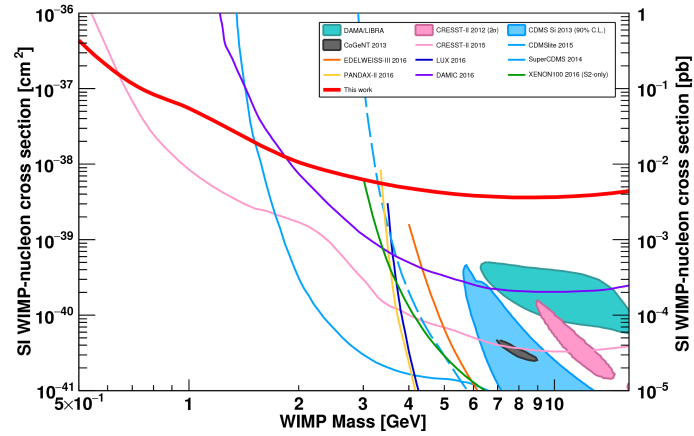


Figure 3. NEWS-G constraints in the spin-independent WIMP-nucleon cross section as a function of the WIMP mass plane (solid red line) [16].

solid red line [16]. New constraints for masses below 0.6 GeV are set. The recoil energy spectrum used to derive the sensitivity to light DM is based on standard assumptions of the DM-halo model.¹

4 Developments in sensor design

The design of the sensor and its support structure are crucial for the detector performance, as they directly affect the electric field strength and uniformity. In the following, recent developments on this topic are discussed.

4.1 Single-anode sensors

The anode support structure, in the simplest case consisting of a grounded rod, affects the electric field homogeneity and, thus, the homogeneity of the detector response. This is improved

¹DM density $\rho_{DM} = 0.3$ GeV/cm^3 , galactic escape velocity $v_{\text{esc}} = 544$ km/s , asymptotic circular velocity $v_0 = 220$ km/s .

with the development of support structures with correction electrodes, more recently through the development of the resistive glass electrode [17].

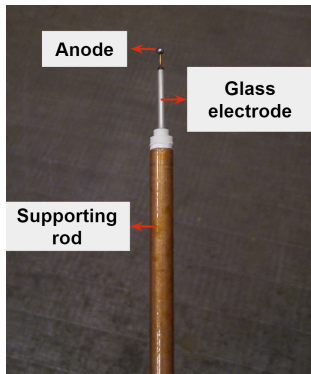


Figure 4. Module with a cylindrical glass correction electrode [17].

In figure 4, the constructed module is presented, composed of a $\varnothing 2$ mm anode made of stainless steel. The glass tube has a length of 20 mm and the distance between the tube and the anode surface is 3 mm. The module was tested in a $\varnothing 30$ cm spherical, stainless steel vessel, supported by a copper rod with a 4 mm (6 mm) inner (outer) diameter.

The electric field homogeneity was investigated using an ^{55}Fe source placed inside the detector. The position of this collimated source could be modified during detector operation. Data were collected with the source located at 90° and 180° to the grounded rod and the distribution of signal amplitude is shown in figure 5(a), demonstrating similar response in both cases and, thus, improved uniformity.

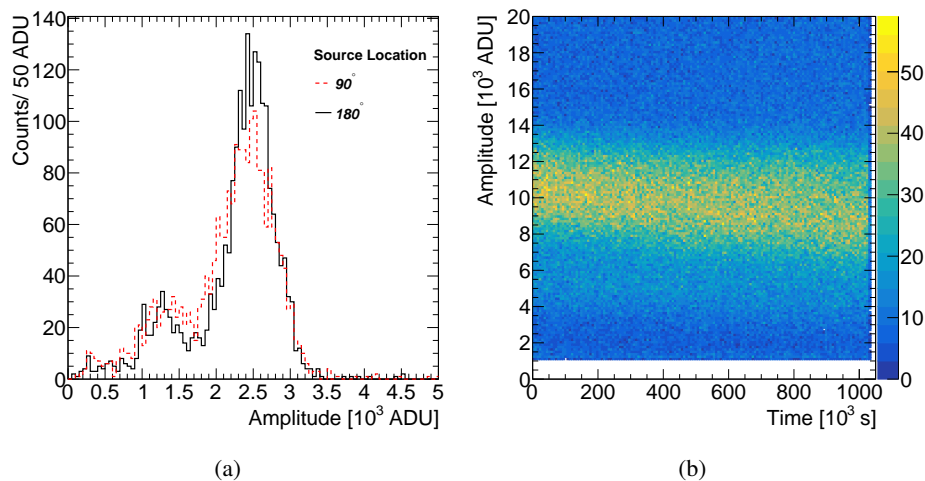


Figure 5. (a) Pulse amplitude distribution for 5.9 keV X-rays from an ^{55}Fe source located inside the detector placed at zenith angle of 90° and 180° , relative to the grounded rod. The detector is filled with He:Ar:CH₄ (92%:5%:3%) at 1 bar. (b) Pulse amplitude as a function of time using a detector filled with 2 bar of He:Ar:CH₄ (87%:10%:3%). Both figures from ref. [17].

The detector operation stability was tested using He:Ar:CH₄ (87%:10%:3%) at 2 bar, introduced using a filter to remove oxygen and water vapour. The 6.4 keV X-ray fluorescence of the ^{55}Fe K-line, induced by environmental γ -rays and cosmic muons, was used to monitor the gas gain as a function of time, as shown in figure 5(b), for 12 days of continuous data-taking. The detector was stable throughout the entire period, with no spark-induced gain variations. The observed decrease of the pulse amplitude in the timescale of days is the result of the gradual introduction of contaminants in the gas volume.

4.2 Multi-anode sensors

One of the challenges towards development of large size spherical proportional counters is the interdependence of the detector gain and the electron drift velocity, in particular at large radii, through the anode electric field in the single-anode sensor. By increasing the electric field of the anode the ionisation electrons at large radii would be efficiently collected, but could lead to breakdown during the avalanche creation, while an electric field providing an acceptable gas gain could be inefficient for the effective collection of the charges.



Figure 6. ACHINOS with 11 balls of $\varnothing 2$ mm constructed using 3D printing [18].

For this reason, ACHINOS [18] — a new multi-anode sensor — is being developed, composed of multiple anode balls equidistantly placed on a virtual spherical surface and all biased at the same potential, as shown in figure 6. Collectively, this leads to an increased electric field strength at large radii, while maintaining the ability to reach high gain operation provided by the individual anode diameter. For example, an ACHINOS sensor with 11 anodes distributed on a $\varnothing 36$ mm sphere produces approximately 9 times larger electric field at large radii, with respect to a single $\varnothing 2$ mm anode at the same bias voltage [18]. This development paves the way for large detector operation under high pressure.

5 A large size spherical proportional counter with compact shielding

The next phase of the experiment builds on the experience acquired from the operation of SEDINE at LSM and consists of a low-background $\varnothing 140$ cm spherical proportional counter at the centre of a new compact shielding. The spherical proportional counter comprises two hemispheres made of Aurubis C10100 copper, with a purity of 99.99%, that were electron beam welded together. The shielding consists of a shell with 3 cm of archaeological lead and 22 cm low-activity lead, which is placed inside a 40 cm thick polyethylene shield, as shown in figure 7. Initial commissioning of the spherical proportional counter took place at LSM and, subsequently, the detector was transferred to SNOLAB, with an overburden of 6000 m water equivalent, for the main physics run. These improvements are expected to lead to significant background reduction, relative to that of SEDINE, and will allow sensitivity down to cross sections of $O(10^{-41} \text{ cm}^2)$ for masses around 1 GeV. The use of hydrogen and helium-rich targets will enable unprecedented experimental sensitivity down to DM candidate masses of 0.1 GeV.

6 Electroplating for NEWS-G

Recently, it has been shown that even class 1,² oxygen-free copper contains unacceptably large amounts of ^{210}Po and ^{210}Pb [19], significantly deteriorating the experimental sensitivity. Geant4-based simulations [20] for the $\varnothing 140$ cm detector suggested that ^{210}Pb and ^{210}Bi decays would

²Classification according to the American Society for Testing and Materials (ASTM) B170 C10100 standard.

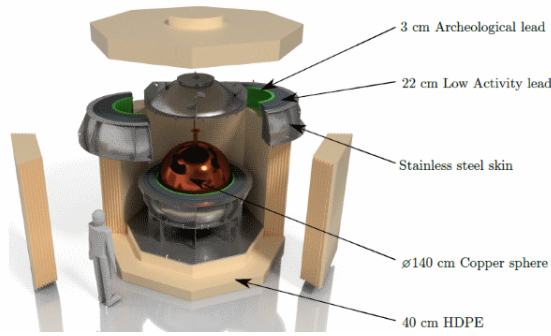


Figure 7. Schematic of the $\varnothing 140$ cm spherical proportional counter and its shielding.

be contributing 4.6 dru,³ below 1 keV, approximately an order of magnitude larger than other background contributions in this energy range. Thus, it was decided to electroplate a 500 μm -thick cladding-type layer of ultra-pure copper on the cathode surface, which is expected to reduce the background in the said energy range by approximately 55%. This procedure uses established techniques [21, 22], and has been implemented by earlier experiments [23].

The electroplating was performed in LSM and the set-up is shown in figure 8. A smaller hemisphere of copper was prepared to act as the anode for electroplating. This smaller hemisphere was suspended concentrically inside the detector hemisphere, separated by an electrolyte of de-ionised water and sulphuric acid. During electroplating, a voltage between the electrodes induces a current through the electrolyte solution. This facilitates reduction reactions at the cathode which result in the deposition of ions from the electrolyte on the cathode surface.

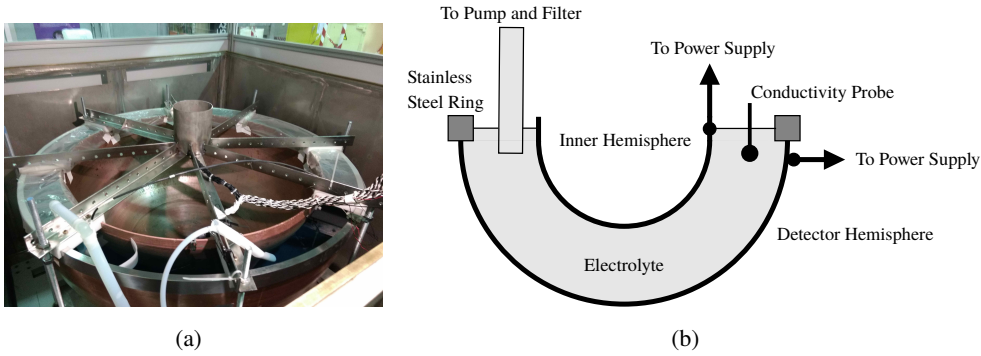


Figure 8. (a) Electroplating set-up showing the detector hemisphere, anode, support structures and fixtures. (b) schematic of the set-up. A pump is installed to provide mechanical mixing, while the attached filter removes particulates greater than 1 μm in size from the electrolyte.

The hemispheres were first cleaned and sanded, to remove raised portions of copper. The surface was then chemically etched using an acidified hydrogen peroxide solution [22]. Subsequently, the surface was electropolished, the opposite process of electroplating, removing (21.2 ± 0.1) μm and (28.2 ± 0.1) μm from each of the detector hemispheres, respectively, to ensure its smoothness, to expose the underlying crystal structure, and to introduce copper ions into the electrolyte.

³1 dru = 1 count/keV/kg/day

The electroplating continued for approximately 15 days for each hemisphere using a pulse reverse current technique [24]. The potential difference used between the anode and the cathode for electroplating was 0.3 V, the established value for electroplating pure copper. From the recorded current, and by assuming uniform deposition of copper, it was estimated that $(502.1 \pm 0.2) \mu\text{m}$ and $(539.5 \pm 0.2) \mu\text{m}$ of copper were plated onto the surface of the two hemispheres, respectively. Finally, the surface was rinsed with water and passivated with a 1% citric acid solution [22]. The achieved plating rate corresponds to approximately 1.3 cm year^{-1} , demonstrating the possibility to electroform a complete sphere underground.

7 Gas purification

The quality of the gas mixture is of paramount importance for the performance of the experiment. Electronegative gas contaminants lead to electron attachment, and, thus, signal reduction and deterioration of energy resolution and background discrimination. Such effects are particularly important in regions of low electric field strength. Gas filtering using Messer Oxisorb or Saes MicroTorr Purifier was introduced to ensure that oxygen and water induced effects are minimised. Figure 9 shows the pulse amplitude for 5.9 keV X-rays measured with a spherical proportional counter filled with filtered and unfiltered gas. Filtering improved the measured resolution (σ/E), from $(21.3 \pm 0.7) \%$ to $(9.4 \pm 0.3) \%$. However, it was found that the filtering process introduces non-negligible amounts of ^{222}Rn . Such behaviour has been previously reported [26–28], and the introduction of a carbon filter to remove the emanated ^{222}Rn is investigated.

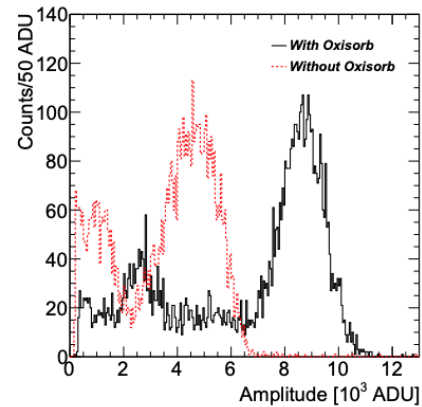


Figure 9. Signal comparison of 5.9 keV X-rays in a spherical proportional counter filled with 600 mbar of He:CH₄ (90%:10%) gas with and without filtering [25].

8 Detector calibration and monitoring

The performance of the detector as a function of time, as well as detailed studies of the detector response at the single electron level, are enabled by the use of a laser-based calibration system [29]. The experimental setup, which incorporates a monochromatic UV laser beam with variable intensity, is shown in figure 10(a). The trigger for data acquisition is provided by the laser signal in a photo detector, allowing for precise measurements of electron transport parameters, e.g. drift time, diffusion coefficients, and electron avalanche gain, as well as trigger efficiency measurements. These studies are complemented with an ^{37}Ar gaseous calibration source for measurements of the gas W-value and Fano factor. The calibration system can be used in parallel with data-taking for physics to monitor the detector response, as shown in figure 10(b).

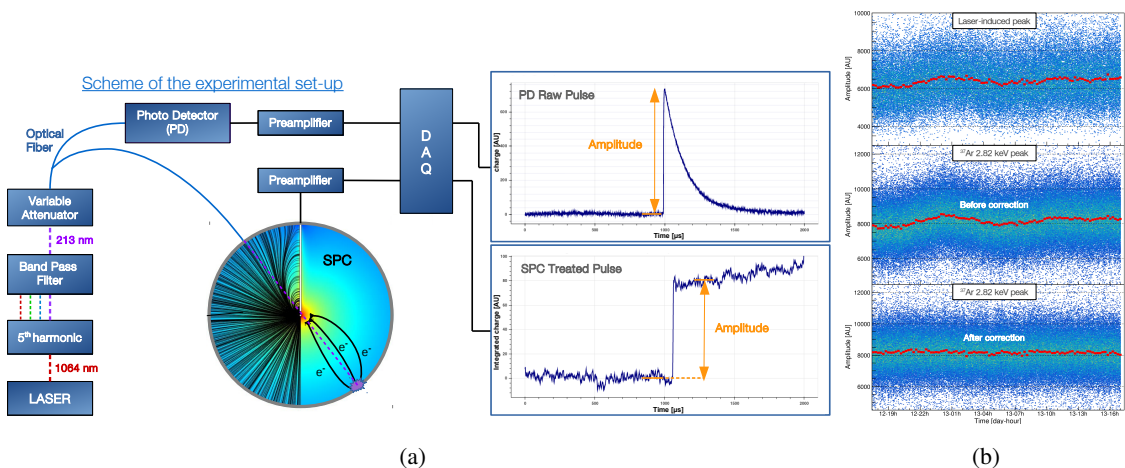


Figure 10. (a) Schematic of the laser-based calibration system. (b) Gain stability monitoring in a spherical proportional counter using a UV laser. The top panel shows the distribution of pulse amplitude as a function time for laser-induced events. The middle (bottom) panel shows the distribution of ^{37}Ar 2822 eV events before (after) correcting for gain variations using the amplitude of laser-induced events. Red markers indicate the centre of a Gaussian fit to amplitude spectra for time slices of 15 min. Both figures from ref. [29].

9 Summary

The spherical proportional counter is a novel gaseous detector offering significant advantages in the search for light dark matter candidates in the range between 0.1 and 10 GeV. The first physics results of the NEWS-G collaboration were obtained using the SEDINE detector, a 60 cm in diameter spherical proportional counter, operating at LSM. These results demonstrate the potential of spherical proportional counters in the search of low-mass DM candidates. A new 140 cm in diameter detector, was constructed and commissioned at LSM during summer 2019, and is currently being installed in SNOLAB. Several improvements, based on the experience from SEDINE, have been incorporated in the design. These include low-activity copper, electroplating a layer of copper onto the inner surface of the detector, and a new, compact shielding. These improvements, together with the developments in sensor design, are expected to lead to substantial improvements in the sensitivity for light DM candidates.

Acknowledgments

This work is supported by the Royal Society International Exchanges and the IPPP Associateship schemes, and by UKRI-STFC through the University of Birmingham Particle Physics Consolidated Grant.

References

- [1] J. Silk et al., *Particle Dark Matter: Observations, Models and Searches*. Cambridge Univ. Press, Cambridge, 2010, [10.1017/CBO9780511770739](https://doi.org/10.1017/CBO9780511770739).

- [2] D. Clowe et al., *A direct empirical proof of the existence of dark matter*, *The Astrophysical Journal Letters* **648** (2006) L109.
- [3] PLANCK collaboration, *Planck 2015 results - xiii. cosmological parameters*, *Astronomy & Astrophysics* **594** (2016) A13.
- [4] J. L. Feng, *Dark Matter Candidates from Particle Physics and Methods of Detection*, *Ann. Rev. Astron. Astrophys.* **48** (2010) 495–545.
- [5] G. Jungman, M. Kamionkowski and K. Griest, *Supersymmetric dark matter*, *Phys. Rept.* **267** (1996) 195.
- [6] O. Buchmueller et al., *The CMSSM and NUHM1 in Light of 7 TeV LHC, $B_s \rightarrow \mu^+ \mu^-$ and XENON100 Data*, *Eur. Phys. J. C* **72** (2012) 2243.
- [7] R. Essig et al., *Working Group Report: New Light Weakly Coupled Particles*, in *proceedings of the 2013 Community Summer Study on the Future of U.S. Particle Physics: Snowmass on the Mississippi*, 2013. [1311.0029](#).
- [8] S. Profumo, *GeV dark matter searches with the NEWS detector*, *Phys. Rev.* **D93** (2016) 055036.
- [9] K. Petraki and R. R. Volkas, *Review of asymmetric dark matter*, *Int. J. Mod. Phys. A* **28** (2013) 1330028.
- [10] K. M. Zurek, *Asymmetric Dark Matter: Theories, Signatures, and Constraints*, *Phys. Rept.* **537** (2014) 91.
- [11] SUPERCDMS collaboration, *Dark matter effective field theory scattering in direct detection experiments*, *Phys. Rev.* **D91** (2015) 092004.
- [12] J. Lindhard, V. Nielsen, M. Scharff and P. Thomsen, *Integral equations governing radiation effects (notes on atomic collisions, iii)*, *Kong. Dan. Vid. Sel. Mat. Fys. Med.* **33** (1963) .
- [13] I. Giomataris et al., *A Novel large-volume Spherical Detector with Proportional Amplification read-out*, *JINST* **3** (2008) P09007.
- [14] G. Gerbier et al., *NEWS : a new spherical gas detector for very low mass WIMP detection*, [1401.7902](#).
- [15] I. Savvidis, I. Katsioulas, C. Eleftheriadis, I. Giomataris and T. Papaevangelou, *Low energy recoil detection with a spherical proportional counter*, [1606.02146](#).
- [16] NEWS-G collaboration, *First results from the NEWS-G direct dark matter search experiment at the LSM*, *Astropart. Phys.* **97** (2018) 54, [[1706.04934](#)].
- [17] I. Katsioulas et al., *A sparkless resistive glass correction electrode for the spherical proportional counter*, *JINST* **13** (2018) P11006, [[1809.03270](#)].
- [18] A. Giganon et al., *A multiball read-out for the spherical proportional counter*, *JINST* **12** (2017) P12031, [[1707.09254](#)].
- [19] XMASS collaboration, *Identification of ^{210}Pb and ^{210}Po in the bulk of copper samples with a low-background alpha particle counter*, *Nucl. Instrum. Meth.* **A884** (2018) 157, [[1707.06413](#)].
- [20] GEANT4 collaboration, *GEANT4: A Simulation toolkit*, *Nucl. Instrum. Meth.* **A506** (2003) 250.
- [21] E. Hoppe et al., *Use of electrodeposition for sample preparation and rejection rate prediction for assay of electroformed ultra high purity copper for ^{232}Th and ^{238}U prior to inductively coupled plasma mass spectrometry (icp/ms)*, *J. Radioanal. Nucl. Chem.* **277** (2008) 103.

- [22] E. Hoppe et al., *Cleaning and passivation of copper surfaces to remove surface radioactivity and prevent oxide formation*, *Nucl. Instrum. Methods Phys. Res. A* **579** (2007) 486.
- [23] MAJORANA collaboration, *The Majorana Demonstrator Neutrinoless Double-Beta Decay Experiment*, *Adv. High Energy Phys.* **2014** (2014) 365432.
- [24] M. Chandrasekar and M. Pushpavanam, *Pulse and pulse reverse plating — conceptual, advantages and applications*, *Electrochim. Acta* **53** (2008) 3313.
- [25] P. Knights et al., *Gas and copper purity investigations for NEWS-G*, *J. Phys. Conf. Ser.* **1312** (2019) 012009.
- [26] ARDM collaboration, *Commissioning of the ArDM experiment at the Canfranc underground laboratory: first steps towards a tonne-scale liquid argon time projection chamber for Dark Matter searches*, *JCAP* **03** (2017) 003, [[1612.06375](#)].
- [27] NEXT collaboration, *Measurement of radon-induced backgrounds in the NEXT double beta decay experiment*, *JHEP* **10** (2018) 112, [[1804.00471](#)].
- [28] MUNU collaboration, *Sub MeV Particles Detection and Identification in the MUNU detector*, *Nucl. Instrum. Meth.* **A482** (2002) 408, [[hep-ex/0106104](#)].
- [29] NEWS-G collaboration, *Precision laser-based measurements of the single electron response of spherical proportional counters for the NEWS-G light dark matter search experiment*, *Phys. Rev.* **D99** (2019) 102003, [[1902.08960](#)].